

# Effect of separation points on kinetic parameters in pseudo component separated stage model

Jiakun Dai · Lizhong Yang · Yupeng Zhou ·  
Yafei Wang

Received: 6 April 2009 / Accepted: 5 June 2009 / Published online: 3 July 2009  
© Akadémiai Kiadó, Budapest, Hungary 2009

**Abstract** In pseudo bi-component separated-stage model (PBSM), the effect of the TG value at separation points on the kinetic parameters is studied by residual and theoretical analysis. Simultaneously, a new method to determine the point that is the end of 1st reaction or the initial of 2nd reaction is developed. The investigations have improved the calculation procedure of PBSM. We performed thermogravimetry (TG) analysis on oil tea wood with two-step consecutive model and parallel model. Comparison between the results of the two models and improved PBSM shows well agreements. The influence of different separation points on kinetic parameters is presented.

**Keywords** Kinetic analysis · Thermal decomposition · Lignocellulosic material · PBSM · Mass percentage

## Introduction

The thermo-oxidative degradation of various polymer and lignocellulosic materials has been investigated by TG and DTG simultaneous analysis performed in oxidative atmosphere [1–7]. It was indicated that at the progressive heating of polymer in oxidative atmosphere, three or four complex processes occur successively [4, 5]. Meanwhile, many authors pointed out that the mass losses of lignocellulosic materials decomposition in air showed a two-step decomposition profile, with the first step due to wood devolatilization and the second for char oxidation (e.g., Momoh et al. [6, 7]). Consequently, the kinetic models

consisting of parallel or consecutive reactions of pseudo components have been widely applied to describe the global kinetic behavior in thermo-oxidative degradation [8–15]. Generally, the kinetic parameters are extracted from the differential thermogravimetric (DTG) or thermogravimetric (TG) data by a nonlinear least square algorithm. However, the least square method received some skepticism. According to Varhegyi et al. [16, 17], the systematic errors of the thermal analysis could hinder the mechanistic application of the non-linear least-squares.

Comparatively, Liu et al. [18] developed a new two-step model, named “First Order Pseudo Bi-component Separated-stage Model (PBSM)”, to describe the decomposition behavior of lignocellulosic materials. The model deals with the global mass loss by two pseudo components which decompose, respectively, within two separate temperature ranges, therefore, no nonlinear least square algorithm is required. The model was verified to be suitable for the mass loss processes of variable wood and leaf samples under relatively lower heating rates. The basic idea of PBSM model is based on the experimental observations of that DTG curves at lower heating rates frequently show two nearly separate peaks with relatively narrow overlapping region. Liu’s work regarded the minimum in DTG curve as the point of separation between two mass loss stages. However, if two reactions that occur within a narrow overlapping region, the separation point defined previously is not the accurate one where one reaction ends and the other starts. The mass percentage of this point cannot be defined as  $w_{1\infty}$  and  $w_{20}$ . Therefore, how to select the value of  $w_{1\infty}$  and  $w_{20}$  on TG curve is worth studying.

In the present study, non-isothermal TG analysis on oil tea wood has been studied to understand the decomposition behavior of oil tea wood in air atmosphere. A new method is used to evaluate  $w_{1\infty}$  and  $w_{2\infty}$  by residuals analysis. For

J. Dai · L. Yang (✉) · Y. Zhou · Y. Wang  
State Key Laboratory of Fire Science, University of Science and  
Technology of China, Hefei, Anhui Province 230026, China  
e-mail: yanglz@ustc.edu.cn

the evaluation of  $w_{20}$ , a theoretical derivation is carried out to study the influence of  $w_{20}$  on kinetic parameters of second reaction. Meanwhile, two-step consecutive reaction model and parallel reaction model are both applied on the experimental data so that the way of taking value of  $w_{1\infty}$  in PBSM can be further verified.

## Experimental

The raw material used for experiments is oil tea wood collected from Jiangxi province of China. After being dried for 24 h at 80 °C, the material was cut and then ground. A fraction of the material with dimension in 150–300  $\mu\text{m}$  was used for experiments. The grains of samples were distributed over the open sample pan of 5 mm diameter loosely, with the initial amounts of the samples all kept to be nearly 10 mg. The depth of the sample layer filled in the pan was about 0.5 mm. Thermogravimetric analysis (TGA) under air atmosphere was carried out on thermobalance NET-ZSCH STA 409C, controlled by PC compatible system. In this device the thermocouple was not in contact with the sample directly. The temperature calibration of TGA was performed by Curie Point Standards. In tests, air flow was controlled to be 50 mL/min and the temperature was increased from atmosphere temperature to 750 °C at the heating rates of 5–25 K/min with step of 5 K/min. The experiment reproducibility was proved by reasonable agreement between the data obtained from two runs under the same experimental conditions. The DTG curves extracted from the TG data were smoothed by means of Gaussian smoothing algorithm.

## Results and discussion

The procedure to determine the point of separation

When overlapping reactions occur, it is sometimes difficult to locate on the TG curve an unambiguous point where one reaction ends and the other starts. By use of DTG curve, the temperature corresponding to the minimum point [18, 19], which is shown in Fig. 1. The separation point is defined as  $T_{\text{sep}}$ , at which the corresponding value on TG curve is, respectively, defined as  $w_{1\infty}$  and  $w_{20}$ . In Fig. 1, subscripts onset and offset, respectively, correspond to the initial of reaction and the end of reaction. It is assumed that the initial of overall reaction is  $T_{\text{onset1}}$  and the end of overall reaction is  $T_{\text{offset2}}$ . In PBSM, the initial and residual solid mass fractions corresponding to the two separate reactions are defined, respectively, in the definite lower and higher

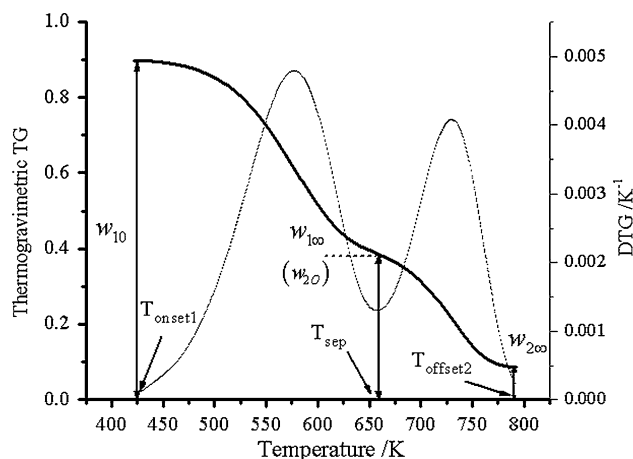


**Fig. 1** Illustration of separation point  $T_{\text{sep}}$ ,  $T_{\text{onset1}}$  and  $T_{\text{offset2}}$  defined in PBSM

temperature ranges, and accordingly the global mass loss kinetics can be expressed as:

$$\begin{cases} \frac{dz_1}{dt} = \frac{A_1}{\beta} \exp(-E_1/RT) f_1(\alpha_1) & T_{\text{onset1}} < T < T_{\text{sep}} \\ \frac{dz_2}{dt} = \frac{A_2}{\beta} \exp(-E_2/RT) f_2(\alpha_2) & T_{\text{sep}} < T < T_{\text{offset2}} \end{cases} \quad (1)$$

In Eq. 1, mass loss fraction  $\alpha_1$  and  $\alpha_2$  are decided by

$$\alpha_1 = \frac{w_{10} - w_1}{w_{10} - w_{1\infty}} \quad (2)$$

$$\alpha_2 = \frac{w_{20} - w_2}{w_{20} - w_{2\infty}} \quad (3)$$

where  $\alpha$  is the sample mass loss fraction and  $w$  is the mass percentage of solid. The subscripts 0 and  $\infty$  refer to the initial and residual amounts, and the subscripts 1 and 2, respectively, correspond to the pseudo components 1 and 2. However, due to reactions that occur within the same temperature range, it is more reasonable to use an extrapolation procedure such as that shown in Fig. 2 to determine approximately where the first reaction starts and the second

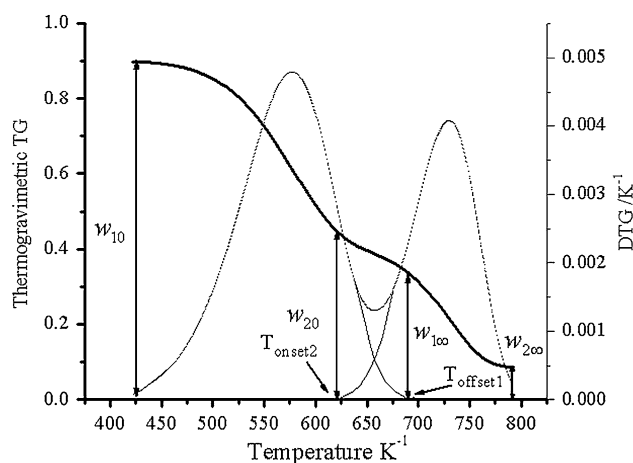


**Fig. 2** Illustration of separation point  $T_{\text{offset1}}$  and  $T_{\text{onset2}}$  defined in PBSM

reaction begins. The mass percentage  $w_{1\infty}$  and  $w_{20}$  need more accurate evaluations. By estimating from Figs. 1 and 2, it is assumed that the temperature at  $T_{\text{offset1}}$  is greater than that at  $T_{\text{sep}}$  by 30 K, and  $T_{\text{onset2}}$  is lower by 30 K. As follow, to sustain this conjectural method, more analytical results are performed.

Evaluation of the offset of first mass-loss reaction  $w_{1\infty}$

A new method to evaluate the mass percentage at the end of first mass-loss reaction accurately is developed here. By taking logarithm of Eq. 1, the following equation is get

$$\ln \frac{d\alpha_1}{dT} = \ln \frac{A}{\beta} - \frac{E}{RT} + n \ln(1 - \alpha_1) \quad (4)$$

for which we regard  $-1/T$  and  $\ln(1 - \alpha_1)$  as predictive variables, and  $\ln d\alpha_1/dT$  as a responsive variable. Generally, when  $w_{1\infty}$  is specified, the mass loss fraction  $\alpha_1$  is decided from Eq. 2, and the kinetic parameters of  $E_1$ ,  $A_1$ , and  $n_1$  can be evaluated from Eq. 4 by linear regression analysis, with a corresponding residual obtained:

$$R = \left( \sum_{i=1}^N (\alpha(i)_{\text{exp}} - \alpha(i)_{\text{cal}})^2 \right) / N \quad (5)$$

where  $N$  is the number of experimental data of the first mass loss reaction. The value of the  $R$  function is related to the quality of fit in regression analysis. Therefore, the more exact  $w_{1\infty}$  is chosen, the smaller value of  $R$  should be given. The kinetic parameters are optimized to achieve a higher quality of fit. By use of the minimum in the functional curve as shown in Fig. 3, it is easy to determine an accurate  $w_{1\infty}$ . The values of  $w_{1\infty}$  are given at different heating rates in Table 1. When the predicted values of  $w_{1\infty}$  are taken by calculation, the corresponding values of  $T_{\text{offset1}}$  can be obtained by use of TG curves in Fig. 6. As

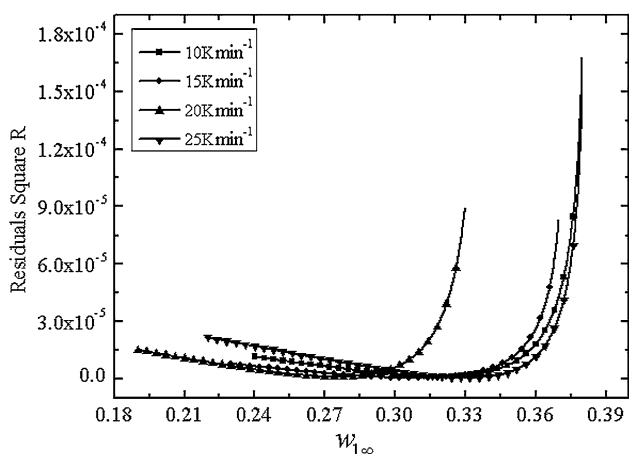


**Fig. 3** The relationship between residual square  $R$  and  $w_{1\infty}$  at different heating rates (10, 15, 20, and 25 K/min)

**Table 1** The mass percentage and temperature at 1st reaction offset point  $T_{\text{offset1}}$  (by calculation) and  $T_{\text{sep}}$

$\beta$ (K/min)	$w_{1\infty}$ ( $T_{\text{sep}}$ )	$w_{1\infty}$ ( $T_{\text{offset1}}$ )	$T_{\text{sep}}$ (K)	$T_{\text{offset1}}$ (K)
10	0.3726	0.3169	645	645 + 27
15	0.3643	0.3080	650	650 + 26
20	0.3277	0.2730	660	660 + 26
25	0.3732	0.3288	665	665 + 23

**Table 2** Comparison of kinetic parameters for oil tea wood with selecting different offset points  $T_{\text{sep}}$  and  $T_{\text{offset1}}$  (heating rates 10, 15, 20, 25 K/min)

$\beta$ (K/min)		$E_1$ (kJ/mol)	$\ln A_1$ ( $s^{-1}$ )	$n_1$
10	$T_{\text{sep}}$	63.7	4.01	0.86
	$T_{\text{offset1}}$	91.6	6.84	1.89
15	$T_{\text{sep}}$	65.9	4.12	0.81
	$T_{\text{offset1}}$	86.9	6.25	1.70
20	$T_{\text{sep}}$	65.4	4.05	0.89
	$T_{\text{offset1}}$	89.2	6.45	1.85
25	$T_{\text{sep}}$	70.3	1.42	0.88
	$T_{\text{offset1}}$	87.5	6.14	1.63

shown in Table 1, the realistic offset point of first reaction  $T_{\text{offset1}}$  is almost greater than  $T_{\text{sep}}$  by 20–30 K. Due to the corresponding minimum of  $R$ , it is reasonable to take value of mass percentage at  $T_{\text{offset1}}$ , when using Eq. 2. In this way, the kinetic parameters can be further extracted. The comparison of kinetic parameters in Table 2 indicates that the deviations of  $w_{1\infty}$  bring the great errors of kinetic parameters.

To enable a visual comparison to be made between the two procedures by  $T_{\text{sep}}$  and  $T_{\text{offset1}}$ , the mathematical Eq. 4 is integrated numerically with the corresponding kinetic constants (in Table 2). Experimental and simulated curves of TG are represented for experiment at 10, 15, 20, and 25 K/min in Figs. 4 and 5. Compared to the  $T_{\text{sep}}$  analysis in Fig. 4, the other kinetic parameters optimized by using point  $T_{\text{offset1}}$  achieve a high quality of fit in Fig. 5.

Evaluation of the onset of second mass-loss reaction  $w_{20}$

By the same method, the onset of second reaction ( $w_{20}$ ) is evaluated, whereas an accurate  $w_{20}$  is difficult to determine from the minimum point in Fig. 6. A set of horizontal lines is shown in this figure, which indicates there is no specific functional relationship between residuals square  $R$  and  $w_{20}$ . Furthermore, the value of  $w_{20}$  may have no influence on the kinetic parameters ( $E_2$ ,  $A_2$ , and  $n_2$ ) of second reaction. The following analyses can sustain this conclusion.

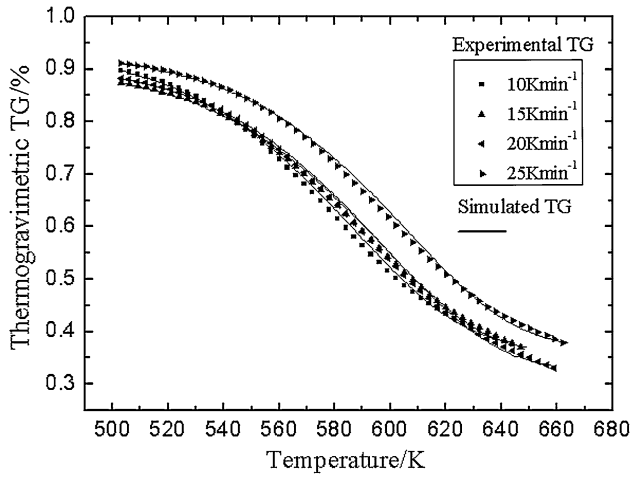


Fig. 4 Comparison of experimental TG in first reaction stage and simulated curves with selecting different offset points  $T_{sep}$

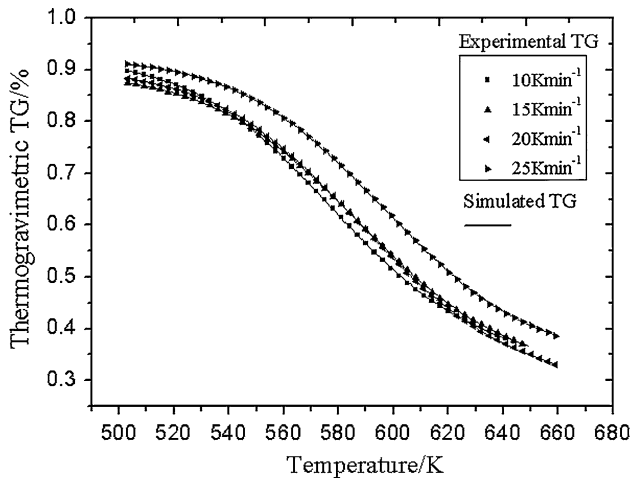


Fig. 5 Comparison of experimental TG in first reaction stage and simulated curves with selecting different offset points  $T_{offset1}$

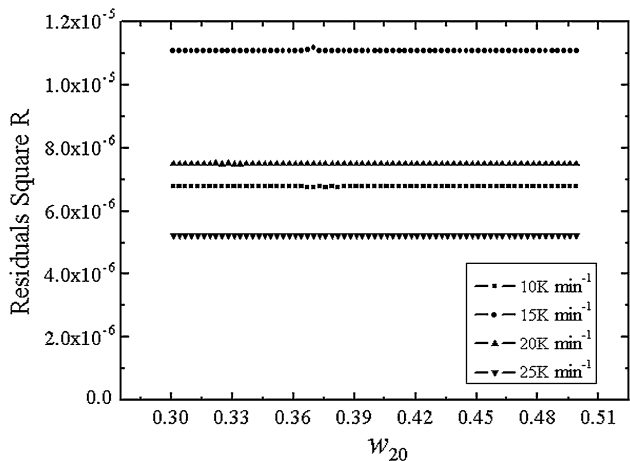


Fig. 6 The relationship between residual square  $R$  and  $w_{20}$  at different heating rates (10, 15, 20, and 25 K/min)

Formula derivation starts from Eq. 1. By taking logarithm of this equation, we can obtain:

$$\ln \frac{d\alpha_2}{dT} = \ln \frac{A_2}{\beta} - \frac{E_2}{RT} + n_2 \ln (1 - \alpha_2) \tag{6}$$

substituting Eq. 3 into Eq. 6:

$$\begin{aligned} \ln \left( d \left( \frac{w_{20} - w}{w_{20} - w_{2\infty}} \right) / dT \right) &= \ln \frac{A_2}{\beta} - \frac{E_2}{RT} \\ &\quad + n_2 \ln \left( 1 - \frac{w_{20} - w}{w_{20} - w_{2\infty}} \right) \\ \ln \frac{-dw/dT}{w_{20} - w_{2\infty}} &= \ln \frac{A_2}{\beta} - \frac{E_2}{RT} + n_2 \ln \left( \frac{w - w_{2\infty}}{w_{20} - w_{2\infty}} \right) \\ \ln \left( -\frac{dw}{dT} \right) - \ln (w_{20} - w_{2\infty}) &= \ln \frac{A_2}{\beta} - \frac{E_2}{RT} + n_2 \ln (w \\ &\quad - w_{2\infty}) - n_2 \ln (w_{20} \\ &\quad - w_{2\infty}) \end{aligned}$$

$$\begin{aligned} \ln \left( -\frac{dw}{dT} \right) &= -\frac{E_2}{RT} + n_2 \ln (w - w_{2\infty}) \\ &\quad + \left( \ln \frac{A_2}{\beta} - (n_2 - 1) \ln (w_{20} - w_{2\infty}) \right) \end{aligned} \tag{7}$$

The activation energy  $E_2$  and reaction order  $n_2$  are calculated from the slope of a plot of  $\ln (-dw/dT)$  versus  $1/T$  and  $\ln (w - w_{2\infty})$ , and the intercept gives the pre-exponential factor. The predictive variables are independent on the value of  $w_{20}$ , so that the corresponding estimation parameters ( $E_2$  and  $n_2$ ) can be evaluated without an accurate  $w_{20}$ . In the case, the pre-exponential factor  $A_2$  is the only kinetic parameter controlled by  $w_{20}$ .

Here,  $w_{20}$  is assumed to be the real mass percentage of second reaction onset. An intercept is given:

$$C = \ln \frac{A_2}{\beta} - (n_2 - 1) \ln (w_{20} - w_{2\infty}) \tag{8}$$

If there is an error in  $w_{20}$ , defined as  $\varphi$ , the other intercept is:

$$C = \ln \frac{A'_2}{\beta} - (n_2 - 1) \ln (w_{20} + \varphi - w_{2\infty}) \tag{9}$$

by subtracting Eq. 8 from Eq. 9, the error of  $A_2$  can be written:

$$\ln \frac{A'_2}{A_2} = (n_2 - 1) \ln (1 + \varphi / (w_{20} - w_{2\infty})) \tag{10}$$

compared to experimental data, a relatively greater error is defined as:

$$\frac{\varphi}{w_{20} - w_{2\infty}} = -0.2 \tag{11}$$

assuming a reasonable reaction order:

$$n_2 = 1.2 \tag{12}$$

substituting Eqs. 11 and 12 into Eq. 10, we can get the error of  $A_2$

$$\frac{A_2'}{A_2} = 1.0377 \approx 1 \tag{13}$$

From Eq. 13, it is found that the relative error of pre-exponential factor due to the deviation of  $w_{20}$  is not more than 4%. Consequently, the effect of  $w_{20}$  on kinetic parameters of second mass loss can be ignored.

Evaluation of the offset of second mass-loss reaction

$w_{2\infty}$

In Eqs. 2 and 3,  $w_{2\infty}$  plays the same role as  $w_{1\infty}$  in controlling the kinetic parameters, and the correlative discussion is also needed by using the same method in “Evaluation of the offset of first mass-loss reaction  $w_{1\infty}$ ” section. From Fig. 7 and Table 3, though  $w_{2\infty}$  has a relatively visible effect on the kinetic parameters of second reaction, however, the computed  $T'_{offset2}$  approximately equals to  $T_{offset2}$ . The previous procedure to determine where is the end of second mass loss reaction in Fig. 1 is acceptable.

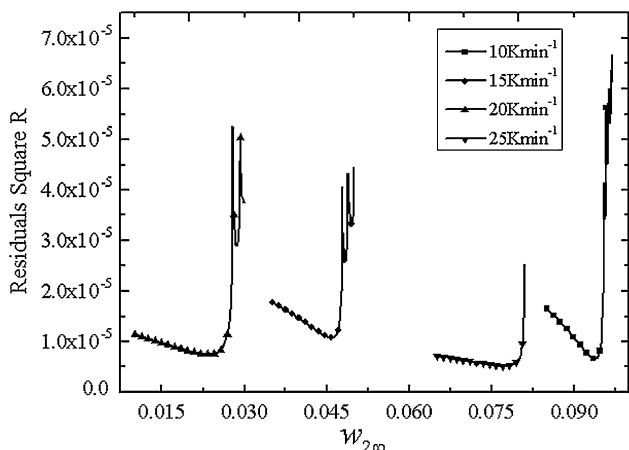


Fig. 7 The relationship between residual square  $R$  and  $w_{2\infty}$  at different heating rates (10, 15, 20, and 25 K/min)

Table 3 The mass percentage and temperature at 2nd reaction offset point  $T_{offset2}$  and  $T'_{offset2}$  (by calculation)

$\beta$ (K/min)	$w_{2\infty} (T_{offset2})$	$w_{2\infty} (T'_{offset2})$	$T_{offset2}$ (K)	$T'_{offset2}$ (K)
10	0.0942	0.0938	775	775 + 2
15	0.0449	0.0459	775	775-1
20	0.0242	0.0235	775	775 + 1
25	0.0758	0.0771	775	775-1

Kinetic analysis for the decomposition of oil tea wood

The decomposition of oil tea wood starts at around 500 K and completes at 773 K (Figs. 8, 9). All the DTG curves show two similar peaks and the separation points at different heating rates are list in Table 1. The characteristic of DTG curves is an indication that the overall reaction contains least two steps.

According to the inspection of literature, parallel reaction model and consecutive reaction model had been proved to be reasonable models to describe the decomposition of biomass because of its two stages characteristics. In order to estimate the kinetic parameters for each pseudo component, a nonlinear least-squares algorithm is applied to the mass loss curves (TG) at different heating rates by single curve analysis. In this study, the NETZSCH Thermokinetics program is used to optimize the kinetic

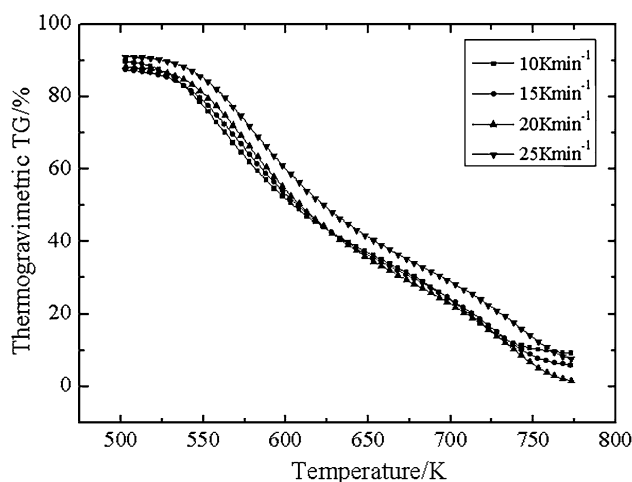


Fig. 8 Experimental TG curves for the experiment with oil tea wood at 10–25 K/min heating rates

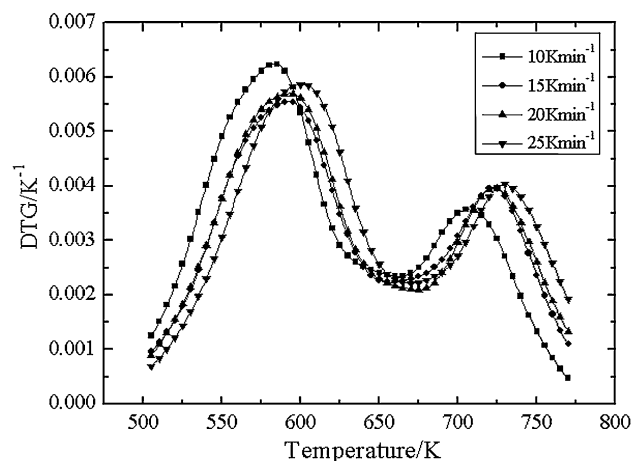
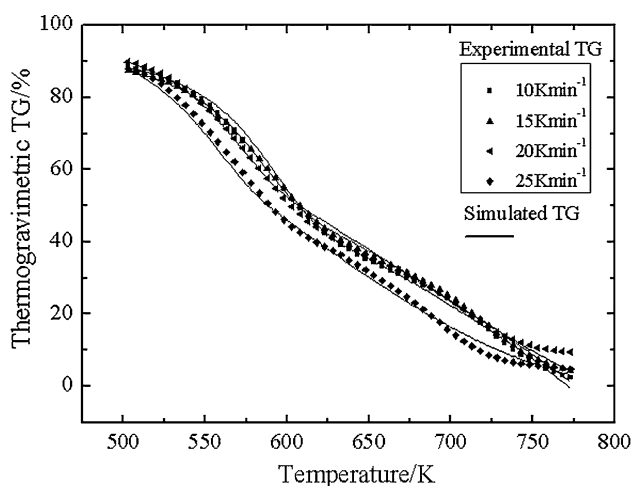
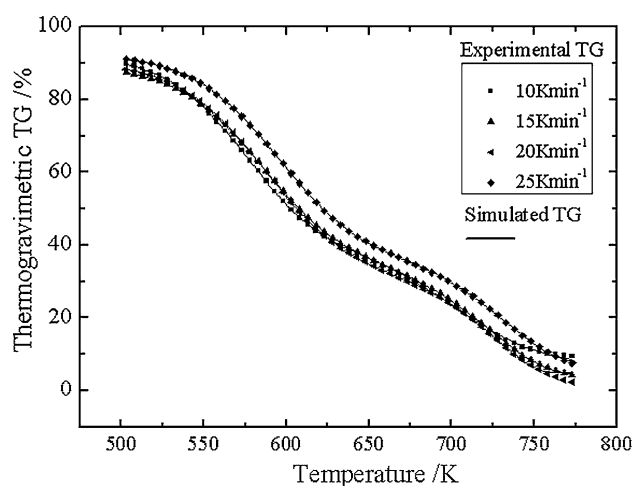


Fig. 9 Experimental DTG curves for the experiment with oil tea wood at 10–25 K/min heating rates



**Fig. 10** Comparison of experimental TG curves of oil tea wood and simulated TG curves by two-step consecutive model assuming  $f(\alpha) = (1 - \alpha)^1$



**Fig. 12** Comparison of experimental TG curves of oil tea wood and simulated TG curves by two-step parallel model assuming  $f(\alpha) = (1 - \alpha)^n$

parameters. The fit between the simulated and experimental data is illustrated in Figs. 10, 11, and 12. As shown, the mechanism function of  $f(\alpha) = (1 - \alpha)^n$  holds better fitting effect than the function of  $f(\alpha) = (1 - \alpha)^1$ . Therefore, the former mechanism function is applied and the extracted kinetic parameters are shown in Table 4. The kinetic parameters by using consecutive model and parallel model are hardly changing with increase of heating rate, which indicates the two models are relatively successful to describe the reaction process. Therefore, it is reasonable to regard kinetic parameters ( $E_1$ ,  $A_1$ , and  $n_1$ ) in Table 4 as good benchmark for the rating of the PBSM model as can be seen from the calculated parameters (Table 2). When defining the mass percentage at  $T_{\text{offset1}}$  is  $w_{1\infty}$ , the simulated kinetic parameters in Table 2 are nearly equal to the

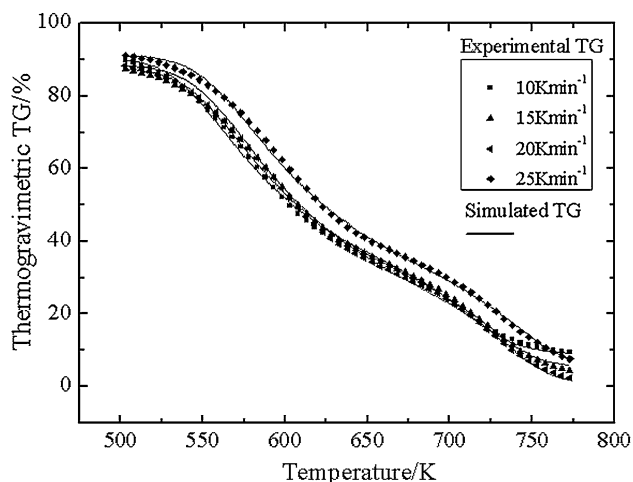


**Fig. 11** Comparison of experimental TG curves of oil tea wood and simulated TG curves by two-step consecutive model assuming  $f(\alpha) = (1 - \alpha)^n$

**Table 4** Comparison of kinetic parameters for decomposition of oil tea wood by two-step consecutive reaction model and parallel reaction model

$\beta$ (K/min)	$E_1$ (kJ/mol)	$\ln A_1$ ( $s^{-1}$ )	$n_1$	$E_2$ (kJ/mol)	$\ln A_2$ ( $s^{-1}$ )	$n_2$	
10	Consecutive	86.3	5.52	1.54	125.8	6.97	1.14
	Parallel	86.0	5.49	1.25	125.0	6.81	0.99
15	Consecutive	83.7	5.40	1.35	114.2	6.16	1.00
	Parallel	84.0	5.43	1.35	112.2	6.00	0.94
20	Consecutive	86.0	5.73	1.44	128.7	7.35	1.00
	Parallel	86.6	5.79	1.48	126.2	7.14	0.67
25	Consecutive	88.1	5.92	1.40	131.7	7.60	1.00
	Parallel	88.6	5.97	1.42	130.3	7.48	0.88

values in Table 4. It is farther indicated that selecting the value of  $w_{1\infty}$  at  $T_{\text{offset1}}$  is more reasonable with comparison of  $T_{\text{sep}}$ .

However, as indicated in previous work [18], the basic idea of PBSM assumed that the pseudo components decompose, respectively, in two separate temperature regions. Therefore, when the decomposition of fractions overlapping region presents extensively, the application of PBSM is limited. Meanwhile, the investigation of separation points' effect on kinetic parameters in this article is only based on the experiment of oil tea wood. The effect of the decomposition of fractions overlapping region on kinetic parameters is ignored, so the corresponding problem motivates the need further investigations.

## Conclusions

In this article, decomposition of oil tea wood has been studied by means of non-isothermal thermogravimetric analysis in air atmosphere at 10–25 K/min heating rates. For the common analysis of the TG measurements run, a satisfactory fit is obtained with consecutive model and parallel model. Compared to these successful models, the procedure of PBSM is further studied. By use of residual analysis and theoretical analysis, the effects of  $w_{1\infty}$ ,  $w_{20}$  and  $w_{2\infty}$  on kinetic parameters are evaluated. It is summarized in the following: (1) It is reasonable to take value of mass percentage at  $T_{\text{offset1}}$ , when estimating the kinetic parameters; (2) For the experimental data of oil tea wood, the realistic offset point of first reaction  $T_{\text{offset1}}$  is almost greater than  $T_{\text{sep}}$  by 20–30 K at different heating rates; (3) The value of  $w_{20}$  almost has no influence on the kinetic parameters ( $E_2$ ,  $A_2$ ,  $n_2$ ) of second reaction; (4) Regarding the end point of overall reaction as  $T_{\text{offset2}}$  is acceptable.

**Acknowledgements** This research was supported by National Natural Science Foundation of China (Grant No: 50536030) and Program for New Century Excellent Talents in University (NCET-05-0551). The authors deeply appreciate the supports.

## References

1. Scuracchio CH, Waki DA, da Silva MLCP. Thermal analysis of ground tire rubber devulcanized by microwaves. *J Therm Anal Calorim.* 2007;87:893–7.
2. Valkova D, Kislínger J, Pekar M, Kucerik J. The kinetics of thermo-oxidative humic acids degradation studied by isoconversional methods. *J Therm Anal Calorim.* 2007;89:957–64.
3. Dweck J. Qualitative and quantitative characterization of Brazilian natural and organophilic clays by thermal analysis. *J Therm Anal Calorim.* 2008;92:129–35.
4. Thomas PS, Guerbois JP, Russel GH, Briscoe BJ. FTIR study of the thermal degradation of poly(vinyl alcohol). *J Therm Anal Calorim.* 2001;64:501–8.
5. Budrugaec P. Kinetics of the complex process of thermo-oxidative degradation of poly(vinyl alcohol). *J Therm Anal Calorim.* 2008;92:291–6.
6. Momoh M, Eboatu A. Thermogravimetric studies of the pyrolytic behaviour in air of selected tropical timbers. *Fire Mater.* 1996;20:173–81.
7. Blasi CDi, Branca C. Global degradation kinetics of wood and agricultural residues in air. *Can J Chem Eng.* 1999;77:555–61.
8. Meszaros E, Varhegyi G, Jakab E. Thermogravimetric and reaction kinetic analysis of biomass samples from an energy plantation. *Energy Fuels.* 2004;18:497–507.
9. Caballero JA, Font R, Maricilla A. Comparative study of the pyrolysis of almond shells and their fractions, holocellulose and lignin. *Thermochim Acta.* 1996;276:57–77.
10. Font R, Marcilla A, Verdu E, Devesa J. Thermogravimetric kinetic study of the pyrolysis of almond shells and almond shells impregnated with  $\text{CoCl}_2$ . *J Anal Appl Pyrol.* 1991;21:249–64.
11. Di Blasi C, Lanzetta M. Intrinsic kinetics of xylan degradation in inert atmosphere. *J Anal Appl Pyrol.* 1997;40–41:287–303.
12. Di Blasi C, Signorelli G, Di Russo C, Rea G. Product distribution from pyrolysis of wood and agricultural residues. *Ind Eng Chem Res.* 1999;38:2216–24.
13. Varhegyi G, Antal MJ, Jakab E, Szabo P. Kinetic modeling of biomass pyrolysis. *J Anal Appl Pyrol.* 1997;42:73–87.
14. Manya JJ, Velo E, Puigjaner L. Kinetics of biomass pyrolysis: a reformulated three-parallel-reactions model. *Ind Eng Chem Res.* 2003;42:434–41.
15. Chen HX, Liu NA, Fan WC. Two-step consecutive reaction model and kinetic parameters relevant to the decomposition of Chinese forest fuels. *J Appl Polym Sci.* 2006;102:571–6.
16. Varhegyi G, Antal MJ, Szabo P, Jakab E, Hill F. Application of complex reaction kinetic models in thermal analysis. *J Therm Anal Calorim.* 1996;47:535–42.
17. Varhegyi G, Szabo P, Jakab E, Till F. Least squares criteria for the kinetic evaluation of thermoanalytical experiments. Examples from a char reactivity study. *J Anal Appl Pyrol.* 2001;57:203–22.
18. Liu NA, Fan WC, Dobashi R. Kinetic modeling of thermal decomposition of natural cellulosic materials in air atmosphere. *J Anal Appl Pyrol.* 2002;63:303–25.
19. Wendlandt WW. *Thermal analysis.* New York: Wiley; 1986.